ARTICLE
Journal of Cellular Biochemistry 116:1646–1657 (2015)

Journal of Cellular Biochemistry

Reveromycin A-Induced Apoptosis in Osteoclasts Is Not Accompanied by Necrosis

Brittany Mead, Heather Morgan, Alyssa Mann-Knowlton, Laura Tedeschi, Chris Sloan, Spenser Lang, Cory Hines, Megan Gragg, Jonathan Stofer, Kaitlin Riemann, Tyler Derr, Emily Heller, David Collins, Paul Landis, Nathan Linna, and Daniel Jones*

Division of Natural Sciences, Department of Biology, Indiana Wesleyan University, South Washington Street, Marion, Indiana

ABSTRACT

Reveromycin A (RM-A), a small natural product isolated from *Streptomyces* bacteria, is a potential osteoporosis therapeutic in that it specifically induces apoptosis in osteoclasts but not osteoblasts. The purpose of the study presented here was to further elucidate the intracellular mechanisms of RM-A death effects in mature osteoclasts. A specific clone of RAW264.7 murine macrophages that was previously characterized for its ability to acquire an osteoclast nature on differentiation was differentiated in the presence of receptor activator of nuclear factor kappa B ligand (RANKL). Subsequent staining was performed for tartrate-resistant acid phosphatase to confirm their osteoclast character. These osteoclasts were treated with ten micromolar RM-A for 2, 4, 6, 24, and 48 h at a pH of 5.5. Peak apoptosis induction occurred at 4–6 h as measured by caspase 3 activity. Lactate dehydrogenase release assay revealed no significant RM-A-induced necrosis. Western blot analysis of cytoplasmic extracts demonstrated activation of caspase 9 (2.3-fold at 2 h and 2.6-fold at 4 h, each $P < 0.05$) and no significant changes in Bcl-X_L. In nuclear extracts, NFκB levels significantly increased on differentiation with RANKL but then remained constant through RM-A treatment. Over the extended time course studied, RM-A-induced apoptosis in osteoclasts was not accompanied by necrosis, suggesting that RM-A would likely have limited effects on immediate, neighboring bone cell types. This specific cell death profile is promising for potential clinical investigations of RM-A as a bone antiresorptive. J. Cell. Biochem. 116: 1646–1657, 2015.

KEY WORDS: REVEROMYCIN A; OSTEOCLAST; APOPTOSIS; NECROSIS

Central to the health of bone tissue is the appropriate balance between the number of active bone-forming osteoblasts and bone-resorbing osteoclasts. The activity and number of each of these cell types is controlled by multiple factors in the bone micro-environment, including growth factors, hormones, cytokines, as well as chemical and physical stimuli [Rehman and Lane, 2003]. Another aspect of maintaining this balance in the bone-forming unit is the process of apoptosis or programmed cell death. During this process damaged or worn out cells are "neatly" eliminated from a tissue [Chua et al., 2002]. This controlled process is distinct from the process of necrosis in which cells typically respond to acute insult by spilling their contents, initiating inflammation [Alberts et al., 2008]. Cells undergoing apoptosis typically shrink in size, displaying membrane blebbing, chromosome condensation, and nuclear DNA fragmentation [Hengartener, 2000; Chua et al., 2002]. Consequently, how various stimuli in the bone affect apoptosis as well as necrosis in osteoblasts and osteoclasts is an intensive area of osteoporosis research.

Therapies for osteoporosis often target osteoclasts, including the use of bisphosphonates which interfere with actin ring formation as well as initiate apoptosis in osteoclasts [Milner et al., 2004; Russell, 2006; Woo et al., 2008]. Another major approach to osteoporosis treatment includes anabolic, bone-forming treatment to increase the activity and number of osteoblasts. This is typically through the intermittent administration of parathyroid hormone (PTH), either the human recombinant, full-length (1–84) form or the recombinant teriparatide (1–34), peptide form [Borba and Mañas, 2010]. Yet another angle of attack in the battle against osteoporosis involves

Brittany Mead, Heather Morgan, and Alyssa Mann-Knowlton contributed equally to this work.
Conflicts of interest: All authors state that they have no conflicts of interest.

*Correspondence to: Daniel Jones, Division of Natural Sciences, Indiana Wesleyan University, 4201 South Washington Street, Marion, Indiana 46953. E-mail: dan.jones@indwes.edu

Manuscript Received: 29 January 2015; Manuscript Accepted: 2 February 2015
Accepted manuscript online in Wiley Online Library (wileyonlinelibrary.com): 9 March 2015
DOI 10.1002/jcb.25125 • © 2015 Wiley Periodicals, Inc.

pairing of anabolic and antiresorptive therapies in combination. Studies in men and women with osteoporosis who received PTH in combination with one of the bisphosphonates, alendronate, show that the action of alendronate to continually inhibit bone resorption interferes with the ability of PTH to increase bone mineral density [Black et al., 2003; Finkelstein et al., 2003; Woo et al., 2008]. Consequently, antiresorptives with mechanisms of action different than bisphosphonates which accumulate in bone need to be developed to improve the efficacy of combination therapies [Woo et al., 2008; Draenert et al., 2012].

A natural product from *Streptomyces*, reveromycin A (RM-A), has been shown to reduce bone resorption in vitro and in vivo by specifically inducing apoptosis of osteoclasts and not osteoblasts or osteoclast precursors [Woo et al., 2006; Stern, 2007]. The osteoclast targeting action of RM-A is thought to depend on the acid pH found intimately associated with the mature osteoclast. This pH is thought to favor RM-A′s ability to permeate the membrane [Stern, 2007]. Interference with the acidic microenvironment through vacuolar H+-ATPase inhibitor treatment abolished the apoptotic action of RM-A on osteoclasts. The antibiotic and antifungal RM-A appears to promote apoptosis through inhibition of isoleucyl-tRNA synthetase in osteoclasts [Woo et al., 2006].

In light of the need to develop antiresorptives for combination therapy that utilize non-bisphosphonate mechanisms, we further characterized the death effects of RM-A. We chose to investigate RM-A action on NFκB, a transcription factor known to be of essential importance in the regulation of osteoclast differentiation and resorptive physiology [Lee and Kim, 2003; Kim et al., 2009]. Intracellular proteins belonging to the bcl-2 (B cell leuke mia/lymphoma 2) family are also critical for regulating apoptosis. Some members, such as bcl-2 and Bcl-X_L [Amarante-Mendes et al., 1998] inhibit cell death by blocking cytochrome c release from the mitochondria while others promote cell death by activating procaspases. We evaluated levels of one of the major anti-apoptotic members of this family, Bcl-X_L, to look for decreases in its levels [Alberts et al., 2008]. The work presented here shows that the intrinsic apoptotic pathway is activated by RM-A as evidenced by procaspase 9 cleavage. Nuclear NFκB and cytoplasmic Bcl-X_L levels are unmodified, but most importantly, RM-A apoptosis is not accompanied by necrosis, even during an extended time course of treatment.

MATERIALS AND METHODS

REAGENTS

Phenol red-free α-MEM media powder was from Cell-Gro (Manassas, VA). Deoxyribonucleotides and ribonucleotides were from Sigma–Aldrich (Saint Louis, MO). Fetal bovine serum was from Hyclone (Logan, UT) and was heat-inactivated by treatment at 56 °C prior to use in the media. Charcoal-stripped fetal bovine serum, L-glutamine, penicillin, and streptomycin were all from Invitrogen (Carlsbad, CA). Sodium bicarbonate, RANKL, and reveromycin A were from Sigma–Aldrich. Primary antibodies of rabbit anti-mouse to biotin, β-actin, β-tubulin, phospho IκBα, IκBα, bcl-X_L, NFκB, and cleaved caspase 9, as well as goat anti-rabbit conjugated to HRP were all from Cell Signalling (Danvers, MA).

RAW264.7 CELL CULTURE AND TREATMENT

Phenol red-free α-MEM was completed with 10 mg/L of each of the deoxyribonucleotides and ribonucleotides with the exception of deoxycytidine (11 mg/L). Sodium bicarbonate was added to 2.2 g/L and L-glutamine was adjusted to 2 mM. RAW264.7 clone 6 cells were a kind gift from Dr. Kevin McHugh of the University of Florida, College of Dentistry. Cells were seeded at 2×10^4 cells/cm^2 in 6-well plates with three wells devoted to each condition. Cells were initially grown in the media (pH 7.4) supplemented with 10% heat-inactivated FBS, 1% penicillin/streptomycin at 37 °C, 5% CO_2 in the presence of 50 ng/ml RANKL. Following 72 h media was removed, a PBS wash was performed, and RANKL-containing media (pH 5.5) supplemented with 10% charcoal-stripped FBS, 1% penicillin/streptomycin was added. Osteoclastogenesis was confirmed by fixing a portion of the RANKL-treated cells with 10% formaldehyde and staining for tartrate-resistant acid phosphatase (TRAP) positive cells with the Sigma–Aldrich Leukocyte Acid Phosphatase Kit. Subsequent treatment was for various times with 10 μM reveromycin A or DMSO vehicle (untreated control). The last 15 min of incubation, three of the wells which were grown in the presence of RANKL and supplemented media without reveromycin A were exposed to 0.1% Triton X-100 to serve as a 100% necrosis control: complete lysis was confirmed by visualization under the phase contrast light microscope.

HARVEST, EXTRACT PREPARATION, AND BRADFORD ASSAY

Following the indicated times of treatment, the media for each condition was harvested and centrifuged at 216 × g for 10 min at room temperature. The resulting supernatant was flash frozen and stored at −80 °C until a subsequent LDH release assay. Cells were scraped into PBS, added to the initial pellet from the media centrifugation, and then re-centrifuged as before. This resulting pellet was resuspended in 25 μl of Promega Cell Lysis Buffer. Cytoplasmic extracts were performed by the multiple freeze-thaw technique, according to the manufacturer′s instructions. The resulting cytoplasmic extracts were flash frozen and stored at −80 °C. The NE-PER Nuclear and Cytoplasmic Extraction Reagent Kit of Thermo Scientific (Rockford, IL) was used to make nuclear extracts from the nuclear pellets. Nuclear extract buffer was supplemented with HALT Protease Inhibitor Cocktail according to Thermo Scientific instructions. Nuclear extracts were flash frozen and stored at −80 °C. Protein concentrations of the cytoplasmic and nuclear extracts were determined in duplicate by the Coomassie dye-based Bradford assay using the Pierce-Thermo Scientific method.

CASPASE 3 ACTIVITY ASSAY

The Promega CaspACE colorimetric caspase 3 activity assay (Madison, WI) was performed following the manufacturer′s instructions. Assay reactions were carried out in duplicate for 4 h at 37 °C and then absorbances were read on a UV-visible spectrophotometer at a wavelength of 405 nm. Caspase 3 activity for each treatment group was expressed relative to the RANKL-differentiated group that was not treated with reveromycin A.

LDH RELEASE ASSAY

The harvested culture supernatants were assayed according to the manufacturer′s instructions using a Promega CytoTox 96 non-

radioactive cytotoxicity assay. A red formazan product formed by LDH activity in the cell supernatant acting upon the tetrazolium salt substrate was measured with a UV-visible spectrophotometer at 490 nm. A modification of the protocol was made in which absorbance of product formed in the presence of LDH released from RANKL-differentiated RAW264.7, clone 6 cells completely lysed by 0.1% Triton X-100 treatment was used as the 100% necrosis value. The corresponding absorbance for each of the other conditions was then expressed as a percentage relative to the 100% necrosis control.

WESTERN BLOT ANALYSIS

For cytoplasmic as well as nuclear protein analyses, equal quantities of extract as determined by Bradford assay were loaded per lane, and proteins were separated by Bio-Rad stain-free 12% Tris HCl, denaturing SDS/PAGE. Images of the separated proteins were obtained with a Bio-Rad Gel Doc EZ System and then quantitated utilizing Image J software. Subsequent analysis was by Western blotting using the ECL detection system (GE Healthcare, Pittsburgh, Pennsylvania) as well as the Super Signal West Pico and Femto detection systems (Thermo Fisher Scientific, Rockford, Illinois) for NFκB visualization. Complete transfer of proteins prior to antibody incubations was confirmed by Ponceau S staining. Signals were quantitated by scanning the processed blots and utilizing Image J software.

STATISTICAL TREATMENT OF DATA

Excel was used to calculate standard error of the mean. A two-tailed Student's *t*-test using Microsoft Excel 2007 software was performed to evaluate significant differences between control and treatment groups.

RESULTS

REVEROMYCIN A INDUCES CASPASE 3 ACTIVITY IN RANKL-DIFFERENTIATED RAW264.7 CELLS WHICH REACHES AN EARLY TIME COURSE PEAK AT FOUR TO SIX HOURS OF TREATMENT

The murine macrophage RAW 264.7 clone 6 cells used in this study were generously provided by Dr. Kevin McHugh. The cells were exposed to RANKL for 72 h before tartrate-resistant acid phosphatase (TRAP) staining to ascertain their differentiation status. In the absence of RANKL the cells grew, maintaining independent, spherical shapes (Fig. 1B). In the presence of RANKL, the cells grew in foci, demonstrating multinucleation (Figs. 1C and 1D), consistent with osteoclast-like morphology observed by others [Huang et al., 2006; Woo et al., 2006]. The TRAP-positive staining of these cultures indicated the presence of functional osteoclasts for these experiments. A more complete characterization of the clone from which these cells were propagated was performed by Cuetara et al. (2006). This particular clone expresses the RANKL receptor and on treatment with RANKL differentiates to large, multinucleated cells that express osteoclast-specific TRAP and cathepsin K, β_3 integrin, and calcitonin receptor mRNAs. This clone resorbs mineralized matrix and through cDNA expression profiling, demonstrates expression of many genes characteristic of osteoclastic differentiation [Cuetara et al., 2006]. These cells were treated with a maximum dose of 10 μM reveromycin A (RM-A), the same maximal dose administered as part of in vivo studies [Woo et al., 2006]. Cells were treated with this dose for 2, 4, or 6 h followed by supernatant and cell pellet collection. Supernatants were used to assess necrosis by LDH release. The cell pellets were used to prepare both cytoplasmic and nuclear extracts: cytoplasmic extracts serving as a source of caspase 3 and proteins for Western analysis and nuclear extracts providing proteins for Western blotting analysis. Equal protein quantities of cytoplasmic extract from both untreated and RM-A-treated cells were assessed for executioner caspase 3 activity, an indicator of apoptosis.

An early time course of apoptosis was initiated. Using the in vitro treatment times of others as a guideline [Zhao et al., 2005; Woo et al., 2006], the cells were treated with 10 μM RM-A for 2, 4, and 6 h before subsequent assessment of caspase 3 activity. No change in caspase 3 activity occurred at 2 h of treatment (Fig. 2). However, a 5.1-fold increase over the untreated condition occurred at 4 h ($P < 0.05$) with a 3.7-fold increase at 6 h ($P < 0.05$). The 4 and 6 h apoptosis levels were not significantly different from one another. This represents the first published report of caspase 3 activity in response to RM-A exposure in RAW264.7 cells. This data is consistent with data of others [Woo et al., 2006]. In that study no caspase 3 data was reported for the RAW264.7 cell line; however, purified osteoclasts were treated for 4 h with 1 μM RM-A to induce apoptosis as measured by fold-induction of caspase 3 activity. This caspase 3 data suggests that apoptosis reaches the initial peak of the execution phase at 4–6 h of treatment (Fig. 2).

REVEROMYCIN A INDUCES APOPTOSIS WITHOUT ANY SIGNIFICANT NECROSIS DURING AN EARLY TIME COURSE IN RANKL-DIFFERENTIATED RAW264.7 CELLS

In determining the actions of RM-A on bone cells, previous studies have focused on determining viability through the 3-(4,5-dimethyl-2-thiazolyl)-2,5-diphenyl-2H tetrazolium bromide (MTT) assay, with purified osteoclasts' survival inhibited at an IC_{50} value of 0.2 μM [Woo et al., 2006]. This effect was highly specific for osteoclasts in that the ED_{50} of RM-A was 100-fold higher for bone marrow cells, calvarial osteoblasts, and others [Woo et al., 2006]. It is known that the MTT assay does not distinguish among apoptosis, necrosis, inhibition of cell growth, or increases in cell numbers of an actively cycling population [McKeague et al., 2003; Lee et al., 2006]. Distinguishing between these two forms of cell death in RAW264.7, clone 6 cells is critical for understanding the RM-A mechanism. During apoptotic death cytosolic contents stay within the plasma membrane boundaries. In contrast necrosis occurs with swelling, bursting, and spillage of the cell components into the extracellular compartment, initiating inflammation [Lee et al., 2006]. To establish death of these osteoclasts by apoptosis alone would be favorable clinically as one of the anti-resorptive features of RM-A. In order to characterize potential necrotic effects of RM-A, we utilized the LDH release assay [Herceg and Wang, 1999; Brennan and Cookson, 2000]. After confirmation of apoptosis via caspase 3 activity assay, the collected supernatants from those cells were assayed for LDH release in order to test the necrotic effects of RM-A. As a positive, 100% necrosis control, three RANKL-treated but RM-A untreated wells were lysed with 0.1% Triton X-100 for 15 min and 100% lysis was

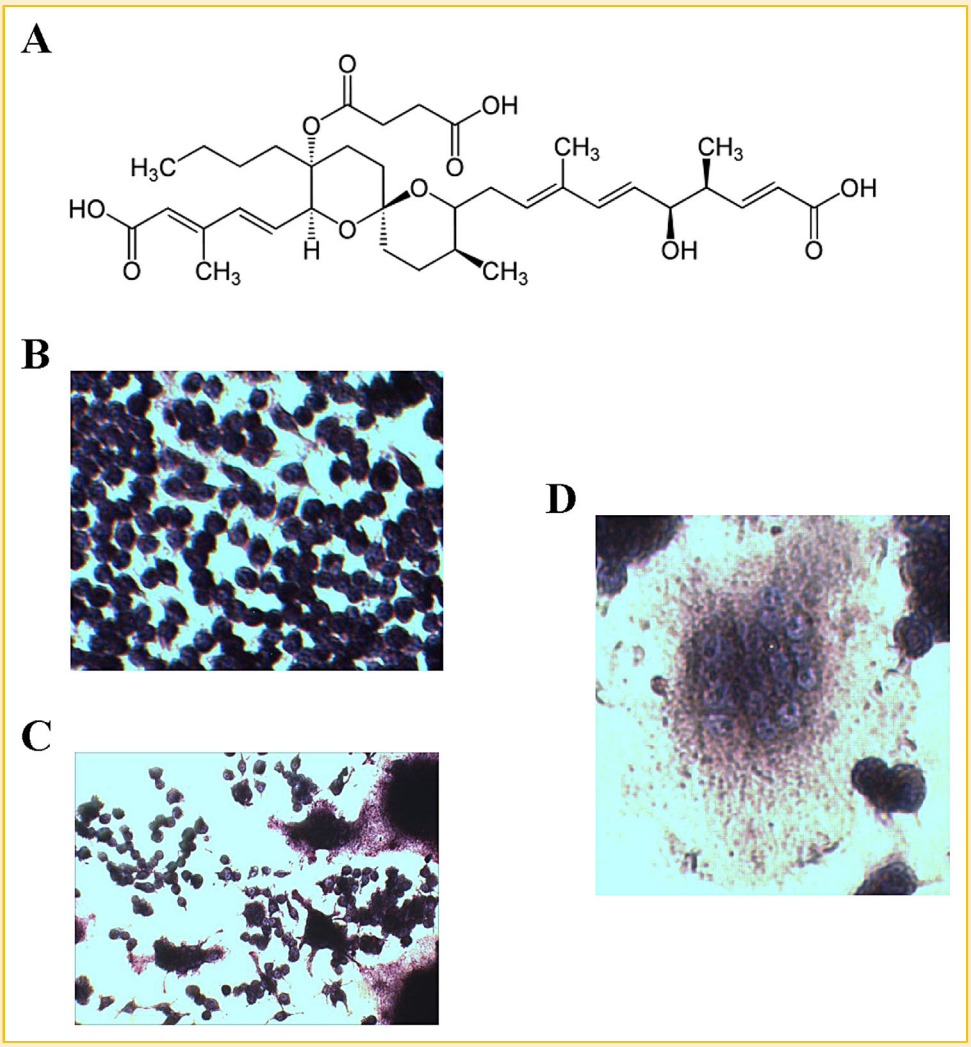

Fig. 1. (A) Chemical structure of the protonated form of RM-A. (B) TRAP-stained RAW 264.7, clone 6 cells in the absence of RANKL, 200 × magnification. (C) TRAP-stained cells following exposure to 50 ng/ml RANKL for 72 h, 150 × magnification. Light purple coloration indicates positive TRAP activity. (D) Multinucleation of TRAP-stained cells following exposure to 50 ng/ml RANKL for 72 h, 300 × magnification.

confirmed through light microscopy. In the untreated (exposed to 1% DMSO vehicle for 6 h) and RM-A-treated wells, no significant necrosis was detected by LDH release when compared to the positive control (Fig. 3A). Average percent necrosis values were 1.7, 3, 2.4, and 3.6% for untreated, 2 h RM-A, 4 h RM-A, and 6 h RM-A, respectively. No significant differences were noted among untreated and the different times of RM-A exposure (Fig. 3B), indicating that death effects from physiologically relevant RM-A levels in osteoclasts are limited to apoptosis only (Fig. 2).

AN EXTENDED TIME COURSE OF REVEROMYCIN A TREATMENT INDICATES NO SIGNIFICANT NECROSIS IN RANKL-DIFFERENTIATED RAW264.7 CELLS

To ascertain that early stages of necrosis were not occurring prior to lysis, an extended time course of treatment was performed out to 48 h of reveromycin A treatment. In addition a parallel extended time course of RANKL in the absence of reveromycin A was performed simultaneously from the same cell batch to understand how much of the observed death effects were from RANKL-induced differentiation alone. This was done because others have established that RANKL-induced osteoclastic differentiation is accompanied by apoptosis [Woo et al., 2002; Song et al., 2015]. Over the extended time course, necrosis as measured by LDH release was the same in the absence versus the presence of 10 μM reveromycin A with the exception of four and 6 h. At those two time points, necrosis was slightly greater in the absence of reveromycin A ($P < 0.05$, Fig. 4A). This strengthens the finding that reveromycin A does not cause significant necrosis in RANKL-differentiated osteoclasts.

The extended time course of 10 μM reveromycin A treatment revealed that apoptosis reached a peak at 6 h (black bars, 3.1-fold increase over RANKL-differentiated, DMSO vehicle control, $P < 0.05$) before diminishing at 24 and further at 48 h (Fig. 4B).

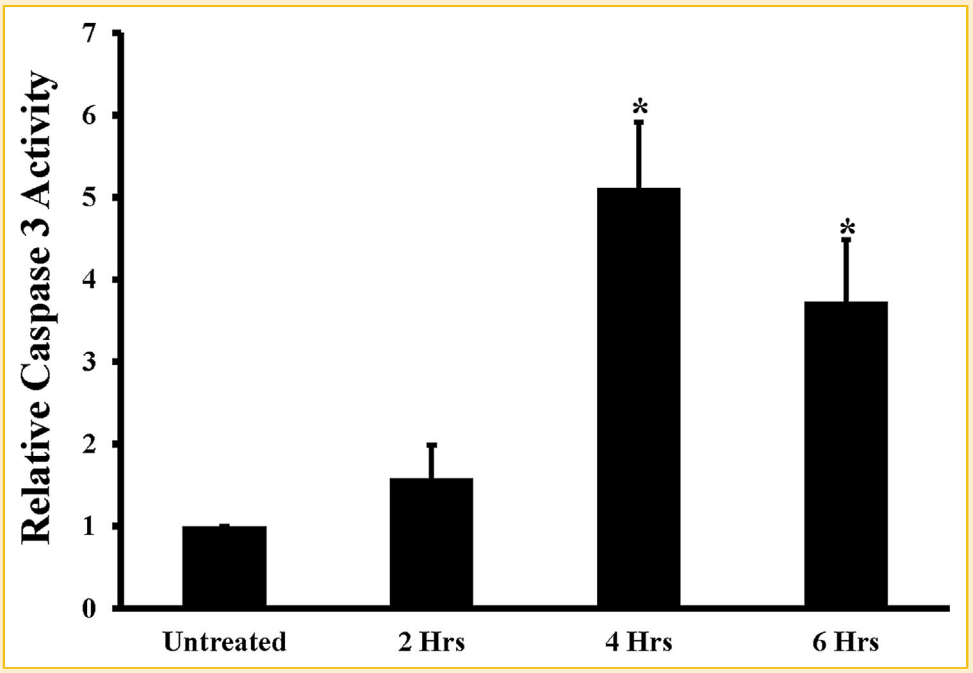

Fig. 2. Early time course of 10 μM RM-A′s apoptotic effect on RANKL-differentiated, RAW264.7, clone 6 cells. Relative caspase 3 activity of untreated (1% DMSO vehicle control) versus 2, 4, and 6 h RM-A-treated cells. Bars indicate mean ± SEM. *$P < 0.05$ compared to untreated control. Results are from three independent experiments, each performed in duplicate.

The parallel time course performed in the absence of reveromycin A showed an expected significant increase in apoptosis on differentiation with RANKL (white bars, 30-fold, NO RANKL versus DMSO, $P < 0.05$). This level of apoptosis did not vary significantly across the RANKL-only time course until the 48 h parallel sample (2.7-fold decrease, $P < 0.05$, Fig. 4B). The samples from the extended apoptotic time courses were assayed in the same caspase 3 assay and the resulting absolute absorbances were reported at 490 nm for direct comparison. When the extended apoptosis time courses are viewed together, it is clear that apoptosis occurs in response to reveromycin A over and above RANKL effects, especially at 6, 24, and 48 h ($P < 0.02$, Fig. 4B).

REVEROMYCIN A EFFECTS ON SELECTED INTRINSIC APOPTOTIC PATHWAY PROTEIN LEVELS IN RANKL-DIFFERENTIATED RAW264.7 CELLS

Reports of others indicate that RM-A activates the intrinsic apoptotic pathway branch as elevated cytochrome c levels have been measured [Woo et al., 2006]. To further investigate this aspect of RM-A action, cleaved caspase 9 levels were detected via Western blotting analysis of the cytoplasmic extract proteins used for the caspase 3 analyses above. Cleaved caspase 9 appeared as a doublet on the blot, reflecting the 39 kDa fragment resulting from cleavage of full-length caspase 9 at aspartic acid 368 and the 37 kDa fragment from cleavage at aspartic acid 353 (Fig. 5A). Activated caspase 9 levels increased 2.3-fold at 2 h ($P < 0.05$) and 2.6-fold at 4 h ($P < 0.05$) of reveromycin A treatment before decreasing back to pre-treatment levels at 6 h (Fig. 5B). This earlier time course of activation compared to the caspase 3 activity profile fits the physiological role of caspase 9 as an initiator caspase [Alberts et al., 2008]. This is the first reported analysis of cleaved caspase 9 in reveromycin A-treated osteoclasts.

Bcl-2 protein family members are known to regulate the intrinsic apoptotic pathway [Alberts et al., 2008]. Work by Kim et al., (2009) showed that Bcl-X_L levels but not Bcl-2 nor XIAP were down-regulated during saurolactam-induced osteoclast apoptosis. Oetzel et al. (2000) also demonstrated down-regulation of Bcl-X_L but in BCR-ABL-positive cells in response to the tyrosine kinase inhibitor ST1 571. Bcl-X_L is known to act as a prosurvival protein, specifically inhibiting apoptosis by sequestering the proapoptotic BH3-only Bcl-2 family subclass [Alberts et al., 2008; Zhao et al., 2008]. To further evaluate the mechanism of RM-A′s intrinsic apoptotic pathway activation and to analyze whether RM-A down regulates Bcl-X_L levels as saurolactam does, we performed Western blot analysis of the cytoplasmic extract proteins used for the caspase 3 analyses. Levels of the deamidated form (higher molecular weight band of the Bcl-X_L doublet) did not change significantly over the 6 h time course (Fig. 5C). It is known that deamidation of Bcl-X_L occurs in cells several steps downstream of routine DNA damage. This damage increases the activity of the amiloride-sensitive sodium-hydrogen exchanger isoform 1, which in turn increases intracellular pH and leads to nonenzymatic deamidation of Bcl-X_L. Bcl-X_L altered in this way is less capable of binding and inhibiting proapoptotic Bcl-2 proteins [Zhao et al., 2008]. Levels of the native form of Bcl-X_L did not change either with reveromycin A treatment (Fig. 5C). Hence Bcl-X_L protein levels are not changed as part of the RM-A intrinsic apoptotic action.

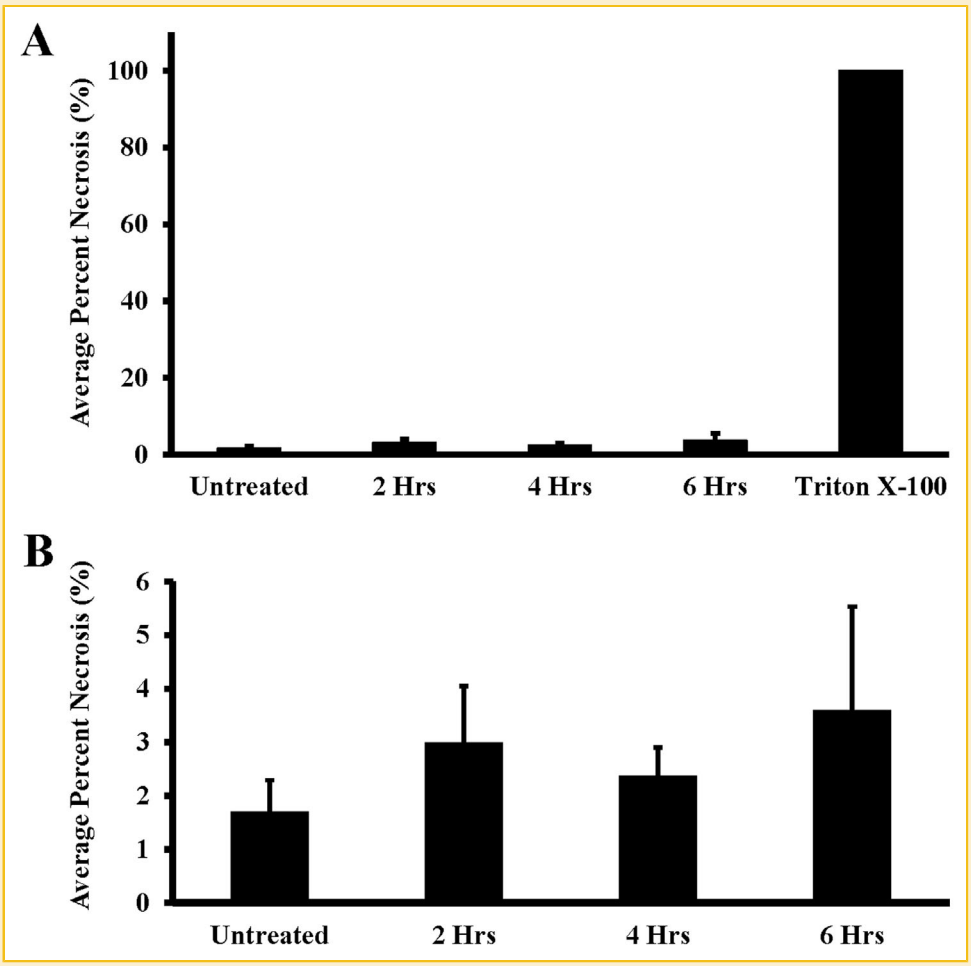

Fig. 3. Measurement of LDH release from RANKL-differentiated RAW264.7, clone 6 cells after 10 μM RM-A treatment. (A) Absorbance of product formed in the presence of LDH released from cells completely lysed by 0.1% Triton X-100 treatment was used as the 100% necrosis value. The corresponding absorbance for each of the other conditions was then expressed as a percentage relative to the 100% necrosis control. Results are from four independent experiments corresponding to experiments in which apoptosis was confirmed via caspase 3 activity assay, each performed in duplicate. Untreated refers to RANKL-differentiated cells exposed to 1% DMSO vehicle for 6 h. (B) Results of panel A graphed without the positive necrosis control to facilitate demonstration of the relative necrosis among the test conditions. Note the consequent change in scale of the *y*-axis compared to that of panel A.

REVEROMYCIN A EFFECTS ON THE NFκB SIGNALLING PATHWAY IN RANKL-DIFFERENTIATED RAW264.7 CELLS

Evidence exists for both survival and apoptotic effects downstream of NFκB activation [Karin and Lin, 2002]. In some cellular contexts the factor behaves as a differentiation and pro-survival signal [Hatada et al., 2000]. In other contexts NFκB functions as a pro-apoptotic signal [Bian et al., 2001]. In osteoclasts, saurolactam- and salinosporamide A-induced apoptosis involve down-regulation of NFκB [Ahn et al., 2007; Kim et al., 2009]. To investigate NFκB′s role in reveromycin A-induced apoptosis in osteoclasts, cytoplasmic inhibitory kappa B alpha (IκBα) levels were analyzed by Western blot analysis. It is known that RANKL binding to RANK triggers a series of events that lead to the phosphorylation of IκBα through IKK with subsequent ubiquitylation and targeting to the proteosome for degradation [Karin and Lin, 2002]. This exposes the nuclear localization signal of NFκB, facilitating its translocation to the nucleus where it can bind its recognition sequence on target genes and activate transcription (Fig. 6A). Cytoplasmic extracts of the untreated and 6 h treated, RANKL-differentiated osteoclasts assayed for caspase 3 activity were also subjected to Western blot analysis, revealing a significant, 3.8-fold decrease in IκBα levels at 6 h of reveromycin A treatment (Fig. 6B and 6 C, $P < 0.001$). Levels of the phosphorylated form of cytoplasmic IκBα were analyzed with an antibody that binds to IκBα phosphorylated at serine 32, serine 36, or both. Levels of phospho IκBα did not change significantly at 2 h of treatment. However, at 4 and 6 h of reveromycin A treatment, levels decreased by 1.4- and 1.9-fold, respectively (each $P < 0.05$ compared to the untreated condition, Fig. 6D and 6 E). With the decreased cytoplasmic IκBα and phosphorylated IκBα levels, we next investigated the levels of nuclear NFκB. Our findings of decreased IκBα and phosphorylated IκBα levels would suggest that NFκB is freed to translocate to the nucleus to activate gene transcription;

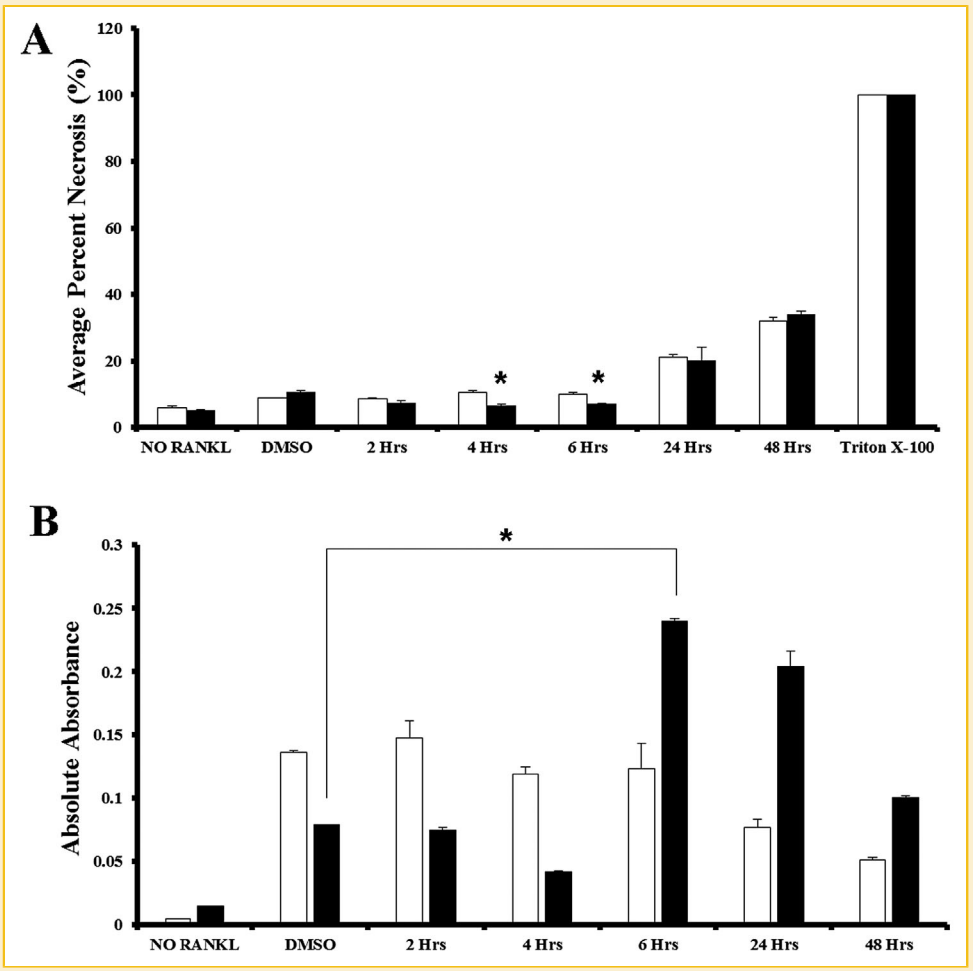

Fig. 4. Extended time course of 10 μM RM-A treatment in RANKL-differentiated RAW264.7, clone 6 cells. (A) Percent necrosis determined relative to cells completely lysed by 0.1% Triton X-100 (100% necrosis). Black bars indicate RANKL-differentiated cells harvested at the indicated times of RM-A treatment. White bars indicate RANKL-differentiated cells not exposed to RM-A but harvested in parallel with the RM-A treated cells. All bars indicate mean ± SEM. *$P < 0.05$ for the following comparisons—RANKL plus 4 h RM-A treatment versus RANKL in the absence of RM-A harvested at the same time point and RANKL plus 6 h RM-A treatment versus RANKL in the absence of RM-A harvested at the same time point. Results are from three independent experiments, each performed in duplicate. (B) Apoptosis determined from caspase 3 assays of equal protein amounts of cytoplasmic extracts from each of the corresponding conditions of panel A. Apoptosis expressed as absolute absorbance of cleaved DEVD-pNA product at 490 nm. Bars as indicated in panel A. *$P < 0.05$ for RANKL plus DMSO vehicle versus RANKL plus 6 h RM-A treatment.

however, Kim et al. have reported inactivation of NFκB during saurolactam-induced apoptosis in the same cell line [Kim et al., 2009].

To account for nuclear NFκB translocation from the action of RANKL alone, we performed Western blot analyses on nuclear extracts from the simultaneous, parallel extended time courses described in the earlier section of results. Consistent with NFκB′s downstream role in the osteoclast differentiation mechanism [Hodge et al., 2011], RANKL differentiation increased nuclear levels of NFκB by 4-fold (Fig. 7A, $P < 0.05$). This level of NFκB did not change over the time course. Normalization of the NFκB signal was performed against total protein because Western blot signal levels of lamin B1, TBP, histone H3, and β-actin loading controls each fluctuated between the "no RANKL" and the RANKL samples. Increases in these loading controls perhaps occurred as a result of multinucleation on differentiation (data not shown). In the simultaneous, parallel extended time course of RANKL plus reveromycin A, RANKL differentiation increased NFκB by 2.1-fold ($P < 0.05$, Fig. 7B). Addition of reveromycin A to RANKL-differentiated RAW264.7 cells resulted in a further very modest increase of 1.7-fold ($P < 0.05$, Fig. 7B). NFκB levels then remained relatively constant on treatment with 10 μM reveromycin A for 2, 4, 6, 24, and 48 h (Fig. 7B). This data differs from the decreased nuclear NFκB observed in saurolactam-induced apoptosis of osteoclasts [Kim et al., 2009].

DISCUSSION

Earlier studies by Woo et al. indicate that RM-A treatment causes significant apoptosis, specifically of osteoclasts in vitro. In vivo studies performed by the same group revealed that RM-A inhibited bone resorption. However, these studies did not address death from

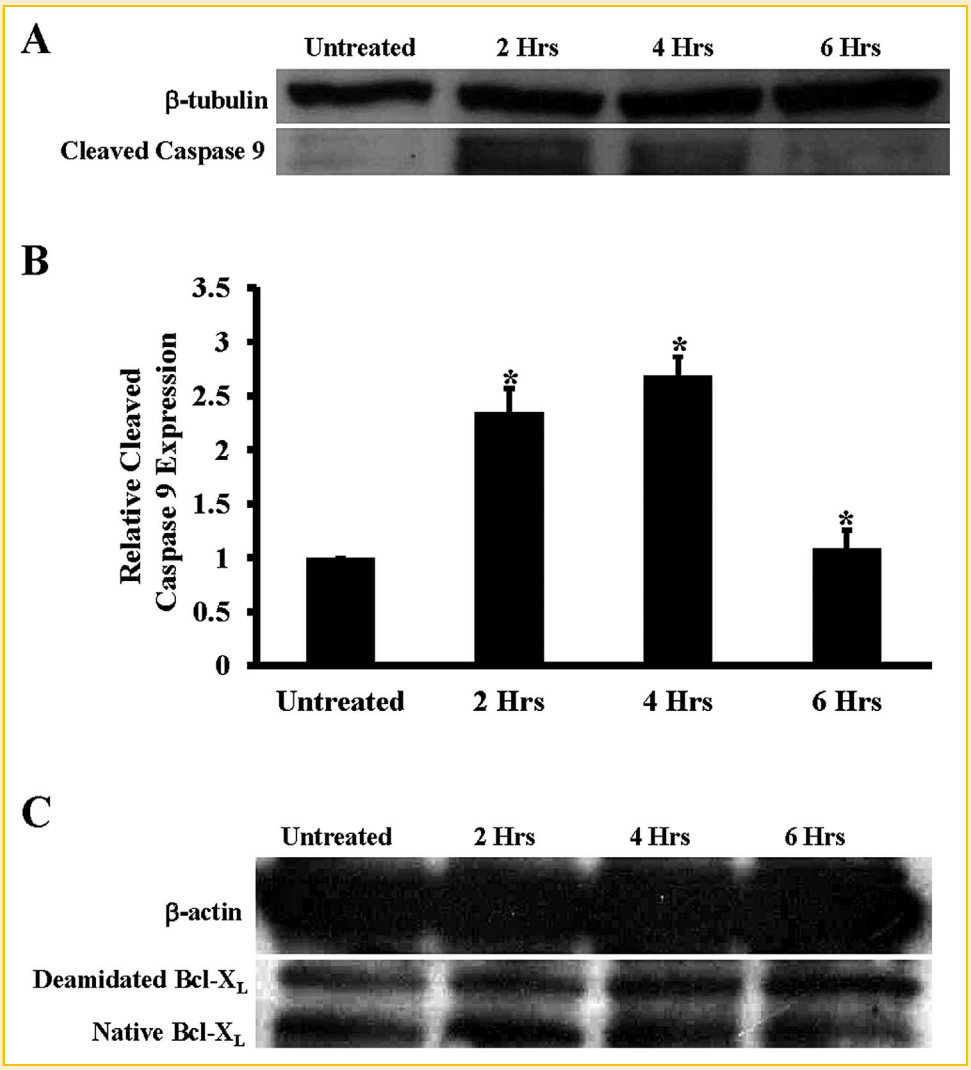

Fig. 5. Measurement of intrinsic apoptotic pathway signalling protein levels in RANKL-differentiated, 10 μM RM-A treated osteoclasts. (A) Western blot analysis of activated (cleaved) caspase 9. A representative blot from one of three independent experiments is shown. (B) The relative caspase 9 expression as determined by Western blot analysis of cytoplasmic extracts from each of the three independent experiments of figure 2. Caspase 9 signal from each lane was normalized to the corresponding β-tubulin signal. The ratio obtained in the untreated condition was set to one and the resulting ratios in the other conditions were each expressed relative to the untreated condition. Error bars indicate mean ± SEM (*$P < 0.05$ for each of the following comparisons: untreated versus 2 h, untreated versus 4 h, and 4 h versus 6 h). (C) Western blot analysis of Bcl-X_L. A representative blot from one of three independent experiments is shown. β-actin was used as an internal loading control. The native form of Bcl-X_L is the higher mobility band of the doublet. The deamidated form is the top band.

necrosis, an effect in which the resulting cytoplasmic and nuclear lysis is known to induce inflammation in surrounding tissues [Iyer et al., 2009]. In our studies RM-A significantly induced apoptosis without accompanying necrosis, a favorable cell death pattern which holds promise for continued development of RM-A as a potential osteoporosis therapeutic. These results suggest that RM-A effects in osteoclasts would produce limited peripheral tissue damage.

The results presented here extend the understanding of RM-A-induced apoptosis in that regulators of apoptosis from treated osteoclasts were examined. RM-A treatment increased levels of active caspase 9, consistent with RM-A-induced cytochrome c levels measured by Woo et al. (2006). One of the pivotal regulators of the intrinsic pathway, Bcl-X_L, is known to be down-regulated in clarithromycin- and azithromycin-induced apoptosis [Mizunoe et al., 2004]. Degradation of Bcl-X_L is also a critical step in hepatic apoptosis that is induced by the pyrrolizidine alkaloids of several plant species worldwide [Ji et al., 2008]. Previous studies have also demonstrated that in addition to its antiapoptotic activity, Bcl-X_L lessens osteoclastic bone-resorbing function through decreased ECM protein production [Iwasawa et al., 2009]. To more completely characterize RM-A′s activation of the intrinsic apoptotic pathway in osteoclasts and to ascertain Bcl-X_L involvement, Bcl-X_L levels were measured. Unlike saurolactam-induced osteoclast apoptosis effects published by Kim et al. (2009) in which native Bcl-X_L was the only form of Bcl-X_L observed, our experiments revealed relatively equal amounts of native and deamidated Bcl-X_L forms. In our RM-A

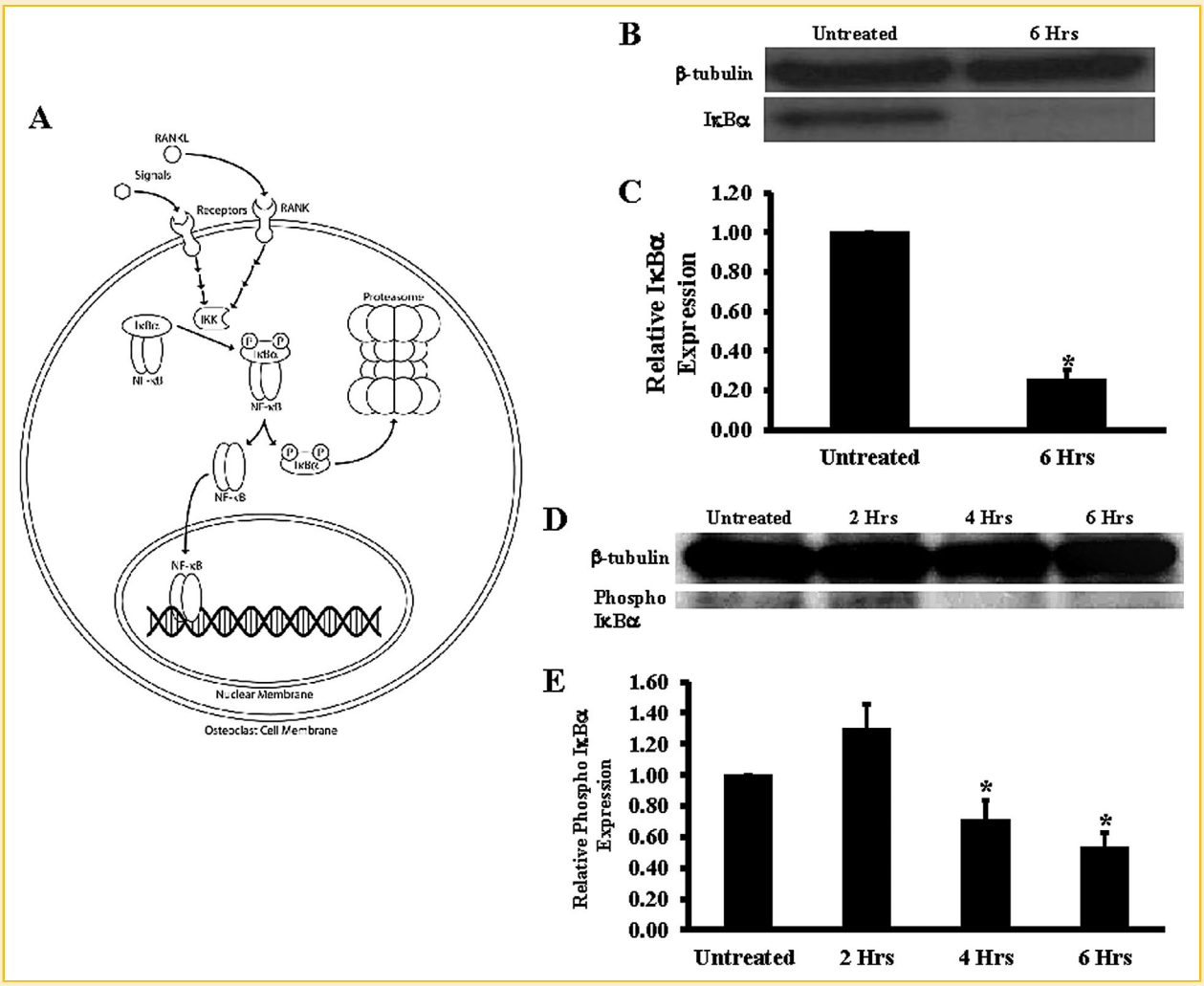

Fig. 6. Western blot analysis of IκBα and phospho IκBα levels in RANKL-differentiated, RM-A treated osteoclasts. (A) Diagram illustrating the NFκB activation pathway (RANKL, receptor activator of NFκB ligand; RANK, receptor activator of NFκB; IKK, inhibitor of κB kinase; IκBα, inhibitor of κBα; P, phosphate group on serine 32 and serine 36 of IκBα; NFκB, nuclear factor kappa B). (B) Western blot analysis of cytoplasmic IκBα. A representative blot from one of three independent experiments is shown. (C) The average IκBα expression as determined by Western blot analysis of cytoplasmic extracts. IκBα signal from each lane was normalized to the corresponding β-tubulin signal. The ratio obtained in the RANKL-differentiated, untreated condition was set to one and the resulting ratio at 6 h of RM-A treatment was expressed relative to the untreated condition. Error bar indicates mean ± SEM (*$P < 0.001$). (D) Western blot analysis of cytoplasmic phospho IκBα. A representative blot from one of three independent experiments is shown. (E) The average phospho IκBα expression as determined by Western blot analysis. Phospho IκBα signal from each lane was normalized to the corresponding β-tubulin signal. The ratio obtained in the RANKL-differentiated, untreated condition was set to one and the resulting ratio at the other conditions was expressed relative to the untreated condition. Error bars indicate mean ± SEM (*$P < 0.05$ for each of the following comparisons: untreated versus 4 h and untreated versus 6 h).

experiments, neither native nor deamidated Bcl-X_L levels changed. Future experiments could address RM-A influence on pro-apoptotic Bax, BIM, BID, Bak, and Bad among others. Interactions of these pro-apoptotic members with Bcl-2, Bcl-X_L, and other survival promoters remain to be determined.

We also examined the involvement of another key signalling molecule in the osteoclast, NFκB. Known to have pleiotropic activity in cells, the NFκB transcription factor modulates differentiation, proliferation, inflammation, and apoptosis. This factor can either enhance transcription of genes that favor survival or can augment transcriptional pathways that lead to cell death [Niu et al., 2010; Oren and Cooks, 2010]. In osteoclasts one of the critical roles NFκB plays is in the differentiation and activation of osteoclast progenitors downstream of RANKL binding to RANK on the progenitor surface [Soysa and Alles, 2009]. In unstimulated osteoclast progenitors, NFκB dimers are sequestered in the cytoplasm by IκB proteins which cover the nuclear localization signal, preventing NFκB transport to the nucleus with the accompanying DNA binding and activation of target genes. When osteoclast progenitors are exposed to RANKL, signalling is activated which leads to the phosphorylation and proteosomal destruction of IκBα, leaving NFκB free to move to the nucleus [Soysa and Alles, 2009]. RM-A-treated osteoclasts exhibited significant decreases in IκBα and phosphorylated IκBα. Additional analysis of nuclear NFκB demonstrated a marked increase on differentiation with RANKL as expected with no further change in levels throughout the 48 h time course of RM-A treatment.

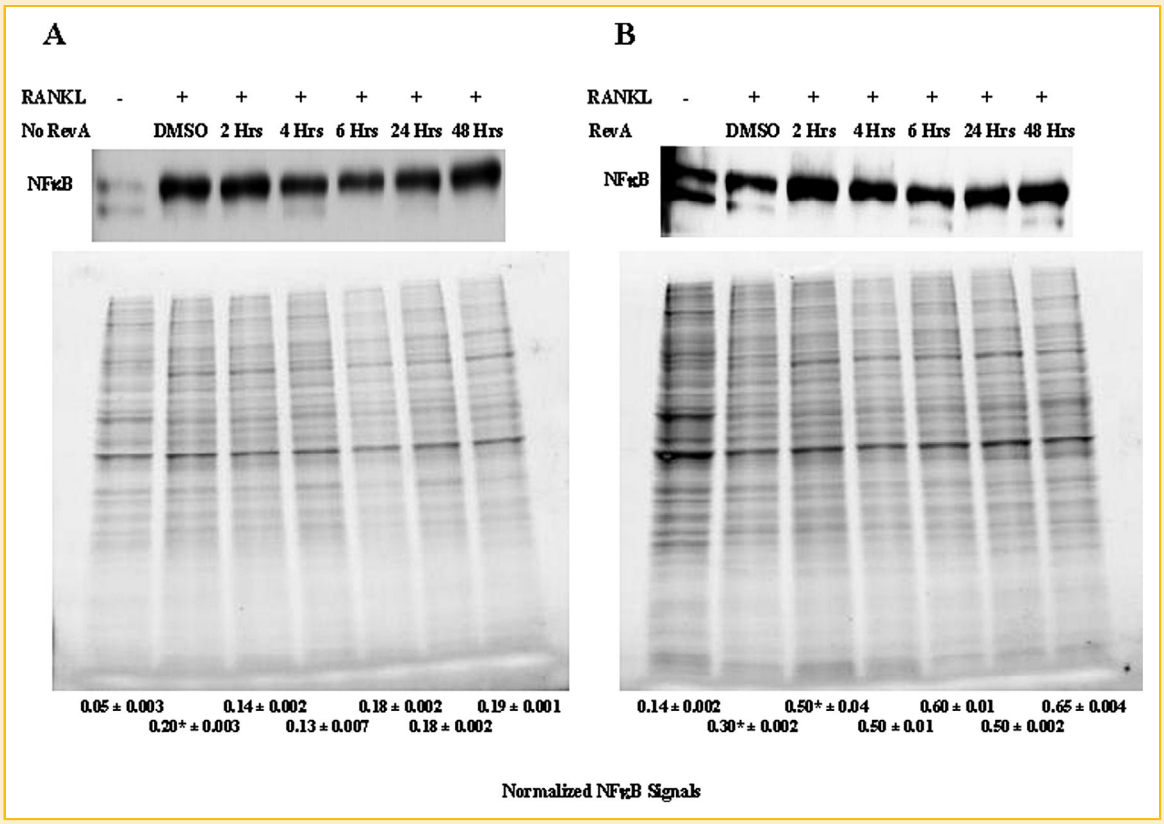

Fig. 7. Western blot analysis of nuclear NFκB levels in RANKL-differentiated, RM-A treated osteoclasts. (A) Western blot analysis of nuclear NFκB levels in RANKL-differentiated, untreated osteoclasts. A representative blot and its corresponding protein gel is shown. NFκB signal from each lane was normalized to the total protein signal. The average normalized NFκB signal ± SEM is shown under each lane. The asterisk indicates $P < 0.05$ for undifferentiated versus differentiated. (B) Western blot analysis of nuclear NFκB levels in RANKL-differentiated, RM-A treated osteoclasts. A representative blot and its corresponding protein gel is shown. NFκB signal from each lane was normalized to the total protein signal. The average normalized NFκB signal ± SEM is shown under each lane. The asterisk indicates $P < 0.05$ for the following comparisons: undifferentiated versus differentiated/untreated and differentiated/untreated versus differentiated/2 h RM-A treatment.

In addition to RM-A, several other antibiotics display actions against osteoclasts. Enoxacin disrupts the normal interaction of the B2 subunit of vacuolar H+ ATPase with microfilaments of the osteoclast cytoskeleton and perturbs post-translational processing and trafficking of multiple osteoclast-specific proteins. Enoxacin does this without inducing apoptosis [Toro et al., 2012]. A bisphosphonate derivative of enoxacin, bis-enoxacin (BE), also blocks the vacuolar H+ ATPase interaction with the cytoskeleton but unlike enoxacin does induce apoptosis, as measured by significant increases in caspase-3 activity. BE inhibited osteoclastic resorption of bone slices in culture and orthodontic tooth movement in rats [Toro et al., 2013]. Both concanamycin A and bafilomycin A1 inhibit vacuolar H+ ATPase, initiating murine osteoclast apoptosis while not affecting survival of osteoblasts from mouse calvaria [Okahashi et al., 1997]. Erythromycin complexed to cyclodextrin (CD-EM) shows promise as a treatment for limiting orthopedic inflammation: CD-EM complexes were noncytotoxic to murine MC3T3 pre-embryonic osteoblasts and RAW 264.7 murine macrophages but did inhibit osteoclast formation [Song et al., 2011]. Tetracycline (TC) and oxytetracycline inhibit osteoclastogenesis and bone resorption of rat bone marrow macrophages in culture. Histomorphometrically tibias of rats treated with TC or oxytetracycline showed a decrease in eroded surface as well as a decrease in the number of osteoclasts per bone surface [Zhou et al., 2010]. Chemically modified tetracyclines promote apoptosis in RAW264.7 cells via increasing the instability of mitochondria [Holmes et al., 2008]. Brefeldin A induces osteoclast apoptosis and hence bone resorption through a p53-dependent mechanism [Niwa et al., 2001].

Others have shown that the natural compound saurolactam, isolated from the plant *Saururus chinensis*, blocked osteoclast differentiation by inhibiting MAP kinase activation and by decreasing the levels of NFATc1, AP-1, and NFκB transcription factors. Saurolactam also induced apoptosis, thus lowering the bone resorptive activity of osteoclasts [Kim et al., 2009]. One variation of this study from the one we report here is that osteoclast progenitors were exposed to saurolactam during differentiation in neutral pH conditions. In our study RM-A exposure commenced in an acidic pH and only after 72 h of continual RANKL exposure. Both aspects of our protocol were performed in an effort to more closely reflect the mature, resorptive osteoclast environment.

Preliminary, comparative examination of the structures of RM-A (Fig. 1A) and saurolactam (Fig. 1B of Kim et al., 2009) shows very limited similarities. The predicted octanol/water partition coefficient, as a measure of lipophilicity, was computed for the two

molecules using the cLogP method [Kenny et al., 2013] found in the OSIRIS molecular property calculator from Actelion labs (http://www.actelion.com). The two values showed considerable difference with the cLogP values of 3.15 and 5.63 for saurolactam and RM-A, respectively. However, both values are within the boundaries for molecules expected to cross the cell membrane. In addition to lipophilicity, size and ionization state factor into the ability of the two molecules to traverse membranes. Both molecules, based on the molecular weight rule of Lipinski′s Rule of 5, would be able to cross the membrane, with RM-A less likely to cross than the small saurolactam [Dhanda et al., 2013]. Considering ionization, at both neutral and acidic pH, saurolactam is unionized whereas RM-A is a dicarboxylate at pH 7.4 and a monocarboxylate at pH 5.5. This last factor, ionization state, may explain the high specificity of RM-A for the osteoclast which resides in an acidic microenvironment: perhaps RM-A is unable to go through the membrane at neutral pH. Others have hypothesized that RM-A specificity may be due to the ionization state of RM-A in the different pH′s found in different tissues [Woo et al., 2006]. The specificity of saurolactam′s effects on different cell types has not been extensively reported; however, one study indicates that saurolactam protects primary cultures of rat cortical cells from glutamate-induced toxicity [Kim et al., 2004].

In summary, RM-A induces osteoclast apoptosis without potentially inflammation-provoking necrosis. The mechanism involves caspase 9 activation, without accompanying changes in anti-apoptotic Bcl-X_L. Unlike saurolactam-induced osteoclast apoptosis, RM-A-induced osteoclast apoptosis is not associated with a change in nuclear NFκB levels. Future investigation should evaluate the death effects of RM-A in other cells of the bone-joint microenvironment, including chondrocytes, synoviocytes, and fibroblast-like synoviocytes. To determine whether RM-A can serve as an osteoporosis therapeutic, it is imperative to test RM-A death effects in these neighboring tissue types at an acidic pH which can occur in non-osteoclast lineages, especially during inflammation [Hu et al., 2012].

ACKNOWLEDGMENTS

We are grateful to Dr. Mark Lipton of the Purdue University Chemistry Department for comparative structural analysis of RM-A and saurolactam. We thank Dr. Kevin McHugh of the College of Dentistry, University of Florida, for the clone 6 RAW264.7 cells. This work was supported by a senior Indiana Academy of Science research grant as well as funding through the Hodson Summer Research Institute. Additional funding was by the Indiana Wesleyan University Lilly Faculty Scholarship Initiative award, the Biology Department, and the Natural Sciences Division of Indiana Wesleyan University.

REFERENCES

Ahn KS, Sethi G, Chao TH, Neuteboom STC, Chaturvedi MM, Palladino MA, Younes A, Aggarwal BB. 2007. Salinosporamide A (NPI-0052) potentiates apoptosis, suppresses osteoclastogenesis, and inhibits invasion through down-modulation of NF-kB-regulated gene products. Blood 110(7): 2286–2295.

Alberts B, Johnson A, Lewis J, Raff M, Roberts K, Walter P. 2008. Apoptosis. In: Anderson M, Granum S, editors. Molecular biology of the cell. New York: Garland Science. pp 1115–1130.

Amarante-Mendes GP, Naekyung Kim C, Huang Y, Perkins CL, Green DR, Bhalla K. 1998. Bcr-abl exerts its antiapoptotic effect against diverse apoptotic stimuli through blockage of mitochondrial release of cytochrome C and activation of caspase-3. Blood 91(5):1700–1705.

Bian X, McAllister-Lucas LM, Shao F, Schumacher KR, Feng Z, Porter AG, Castle VP, Opipari AW, Jr. 2001. NF-kappa B activation mediates doxorubicin-induced cell death in N-type neuroblastoma cells. J Biol Chem 276(52):48921–48929.

Black DM, Greenspan SL, Ensrud KE, Palermo L, McGowan JA, Lang TF, Garnero P, Bouxsein ML, Bilezikian JP, Rosen CJ. 2003. The effects of parathyroid hormone and alendronate alone or in combination in postmenopausal osteoporosis. N Engl J Med 349(13):1207–1215.

Borba VZ, Mañas NC. 2010. The use of PTH in the treatment of osteoporosis. Arq Bras Endocrinol Metabol 54(2):213–219.

Brennan MA, Cookson BT. 2000. Salmonella induces macrophage death by caspase-1-dependent necrosis. Mol Microbiol 38(1):31–40.

Chua C, Chua B, Chen Z, Landy C, Hamdy R. 2002. TGF-b1 inhibits multiple caspases induced by TNF-a in murine osteoblastic MC3T3-E1 cells. Biochim Biophys Acta 1593:1–8.

Cuetera BLV, Crotti TN, O′Donoghue AJ, McHugh KP. 2006. Cloning and characterization of osteoclast precursors from the R AW264. 7 cell line. In Vitro Dev Biol Anim 42:182–188.

Dhanda SK, Singla D, Mondal AK, Raghava GP. 2013. DrugMint: A webserver for predicting and designing of drug-like molecules. Biol Direct 8(1):28.

Draenert GF, Huetzen DO, Kämmerer PW, Palarie V, Nacu V, Wagner W. 2012. Dexrazoxane shows cytoprotective effects in zoledronic acid-treated human cells in vitro and in the rabbit tibia model in vivo. J Craniomaxillofac Surg 40(8):369–374.

Finkelstein JS, Hayes A, Hunzelman JL, Wyland JJ, Lee H, Neer RM. 2003. The effects of parathyroid hormone, alendronate, or both in men with osteoporosis. N Engl J Med 349:1216–1226.

Hatada EN, Krappmann D, Scheidereit C. 2000. NF-kappaB and the innate immune response. Current Opinion in Immunology 12(1):52–58.

Hengartener M. 2000. The biochemistry of apoptosis. Nature 407:770–776.

Herceg Z, Wang ZQ. 1999. Failure of poly(ADP-ribose) polymerase cleavage by caspases leads to induction of necrosis and enhanced apoptosis. Mol Cell Biol 19(7):5124–5133.

Hodge J, Collier F, Pavlos N, Kirkland M, Nicholson G. 2011. M-CSF potently augments RANKL-induced resorption activation in mature human osteoclasts. PLoS One 6(6):e21462.

Holmes S, Smith S, Borthwick L, Dunford J, Rogers M, Bishop N, Grabowski PS. 2008. CMT3 alters mitochondrial function in murine osteoclast lineage cells. Biochem Biophys Res Commun 365(4):840–845.

Hu F, Yang S, Zhao D, Zhu S, Wang Y, Li J. 2012. Moderate extracellular acidification inhibits capsaicin-induced cell death through regulating calcium mobilization, NF-kB translocation and ROS production in synoviocytes. Biochem Biophys Res Commun 424(1):196–200.

Huang H, Ryu J, Ha J, Chang EJ, Kim HJ, Kim HM, Kitamura T, Lee ZH, Kim HH. 2006. Osteoclast differentiation requires TAK1 and MKK6 for NFATc1 induction and NF-kB transactivation by RANKL. Cell Death Differ 13:1879–1891.

Iwasawa M, Miyazaki T, Nagase Y, Akiyama T, Kadono Y, Nakamura M, Oshima Y, Yasui T, Matsumoto T, Nakamura T, Kato S, Hennighausen L, Nakamura K, Tanaka S. 2009. The antiapoptotic protein Bcl-XL negatively regulates the bone-resorbing activity of osteoclasts in mice. J Clin Invest 119:3149–3159.

Iyer SS, Pulskens PP, Sadler JJ, Butter LM, Teske GJ, Ulland TK, Eisenbarth SC, Florguin S, Flavell RA, Leemans JC, Sutterwala FS. 2009. Necrotic cells

trigger a sterile inflammatory response through the Nlrp3 inflammasome. Proc Natl Acad Sci USA 106(48):20388–20393.

Ji L, Chen Y, Liu T, Wang Z. 2008. Involvement of Bcl-XL degradation and mitochondrial-mediated apoptotic pathway in pyrrolizidine alkaloids-induced apoptosis in hepatocytes. Toxicol Appl Pharmacol 231:393–400.

Karin M, Lin A. 2002. NF-kappaB at the crossroads of life and death. Nat Immunol 3(3):221–227.

Kenny PW, Montanari CA, Prokopczyk IM. 2013. CLogP(alk): A method for predicting alkane/water partition coefficient. J Comput Aided Mol Des 27(5):389–402.

Kim SR, Sung SH, Kang SY, Koo KA, Kim SH, Ma CJ, lee HS, Park MJ, Kim YC. 2004. Aristolactam BII of Saururus chinensis attenuates glutamate-induced neurotoxicity in rat cortical cultures probably by inhibiting nitric oxide production. Planta Med 70:391–396.

Kim MH, Ryu SY, Choi JS, Min YK, Kim SH. 2009. Saurolactam inhibits osteoclast differentiation and stimulates apoptosis of mature osteoclasts. J Cell Physiol 221(3):618–628.

Lee ZH, Kim HH. 2003. Signal transduction by receptor activator of nuclear factor kappa B in osteoclasts. Biochem Biophys Res Commun 305:211–214.

Lee WK, Abouhamed M, Thévenod F. 2006. Caspase-dependent and -independent pathways for cadmium-induced apoptosis in cultured kidney proximal tubule cells. Am J Physiol Renal Physiol 291(4):F823–F832.

McKeague AL, Wilson DJ, Nelson J. 2003. Staurosporine-induced apoptosis and hydrogen peroxide-induced necrosis in two human breast cell lines. Br J Cancer 88(1):125–131.

Milner RJ, Farese J, Henry CJ, Selting K, Fan TM, de Lorimier LP. 2004. Bisphosphonates and cancer. J Vet Intern Med 18:597–604.

Mizunoe S, Kadota J, Tokimatsu I, Kishi K, Nagai H, Nasu M. 2004. Clarithromycin and azithromycin induce apoptosis of activated lymphocytes via down-regulation of Bcl-XL. Int Immunopharmacol 4(9):1201–1207.

Niu YL, Zhang WJ, Wu P, Liu B, Sun GT, Yu DM, Deng JB. 2010. Expression of the apoptosis-related proteins caspase-3 and NF-kappaB in the hippocampus of Tg2576 mice. Neurosci Bull 26(1):37–46.

Niwa S, Ishibashi O, Inui T. 2001. Brefeldin A inhibits osteoclastic bone resorption through induction of apoptosis. Life Sci 70(3):315–324.

Oetzel C, Jonuleit T, Götz A, van der Kuip H, Michels H, Duyster J, Hallek M, Aulitzky WE. 2000. The tyrosine kinase inhibitor CGP 57148 (ST1 571) induces apoptosis in BCR-ABL-positive cells by down-regulating BCL-X. Clin Cancer Res 6:1958–1968.

Okahashi N, Nakamura I, Jimi E, Koide M, Suda T, Nishihara T. 1997. Specific inhibitors of vacuolar H(+)-ATPase trigger apoptotic cell death of osteoclasts. J Bone Miner Res 12(7):1116–1123.

Oren M, Cooks T. 2010. NFkB and p53: A life and death affair. Cell Cycle 9(6):1027.

Rehman Q, Lane N. 2003. Effect of glucocorticoids on bone density. Med Pediatr Oncol 41:212–216.

Russell RG. 2006. Bisphosphonates: From bench to bedside. Ann N Y Acad Sci 1068:367–401.

Song R, Liu X, Zhu J, Gao Q, Wang Q, Zhang J, Wang D, Cheng L, Hu D, Yuan Y, Gu J, Liu Z. 2015. RhoV mediates apoptosis of R. Mol Med Rep 11(2): AW264–AW269.

Song W, Yu X, Wang S, Blasier R, Markel DC, Mao G, Shi T, Ren W. 2011. Cyclodextrin-erythromycin complexes as a drug delivery device for orthopedic application. Int J Nanomedicine 6:3173–3186.

Soysa NS, Alles N. 2009. NF-kB functions in osteoclasts. Biochem Biophys Res Commun 378:1–5.

Stern PH. 2007. Antiresorptive agents and osteoclast apoptosis. J Cell Biochem 101:1087–1096.

Toro EJ, Zuo J, Ostrov DA, Catalfamo D, Bradaschia-Correa V, Arana-Chavez V, Caridad AR, Neubert JK, Wronski TJ, Wallet SM, Holliday LS. 2012. Enoxacin directly inhibits osteoclastogenesis without inducing apoptosis. J Biol Chem 287(21):17894–17904.

Toro EJ, Zuo J, Guiterrez A, La Rosa RL, Gawron AJ, Bradaschia-Correa V, Arana-Chavez V, Dolce C, Rivera MF, Kesavalu L, Bhattacharyya I, Neubert JK, Holliday LS. 2013. Bis-enoxacin inhibits bone resorption and orthodontic tooth movement. J Dent Res 92(10):925–931.

Woo KM, Kim HM. 2002. Macrophage colony-stimulating factor promotes the survival of osteoclast precursors by up-regulating Bcl-XL. Exp Mol Med 34(5):340–346.

Woo JT, Kawatani M, Kato M, Shinki T, Yonezawa T, Kanoh N, Nakagawa H, Takami M, Lee KH, Stern PH, Nagai K, Osada H. 2006. Reveromycin A, an agent for osteoporosis, inhibits bone resorption by inducing apoptosis specifically in osteoclasts. Proc Natl Acad Sci USA 103(12):4729–4734.

Woo JT, Yonezawa T, Cha BY, Teruya T, Nagai K. 2008. Pharmacological topics of bone metabolism: Antiresorptive microbial compounds that inhibit osteoclast differentiation, function, and survival. J Pharmacol Sci 106: 547–554.

Zhao H, Ross FP, Teitelbaum SL. 2005. Unoccupied alpha(v) beta3 integrin regulates osteoclast apoptosis by transmitting a positive death signal. Mol Endocrinol 19:771–780.

Zhao R, Follows GA, Beer PA, Scott LM, Huntly BJP, Green AR, Alexander DR. 2008. Inhibition of the Bcl-XL deamidation pathway in myeloproliferative disorders. N Engl J Med 359:2778–2789.

Zhou X, Zhang P, Zhang C, An B, Zhu Z. 2010. Tetracyclines inhibit rat osteoclast formation and activity in vitro and affect bone turnover in young rats in vivo. Calcif Tissue Int 86(2):163–171.